Suppression of heavy-truck driver-seat vibration using sliding-mode control and quantitative feedback theory

N I Rajapakse*, **G S Happawana,** and **Y Hurmuzlu**
Department of Mechanical Engineering, Southern Methodist University, Dallas, Texas, USA

The manuscript was received on 27 October 2005 and was accepted after revision for publication on 21 March 2007.

DOI: 10.1243/09596518JSCE216

Abstract: The current paper presents a robust control method that combines sliding-mode control (SMC) and quantitative feedback theory (QFT) for designing a driver seat of a heavy vehicle to reduce driver fatigue. A mathematical model is considered to analyse tracking control characteristics through computer simulation in order to demonstrate the effectiveness of the proposed control methodology. The SMC is used to track the trajectory of the desired motion behaviour of the seat. However, when the system enters into sliding regime, chattering occurs owing to switching delays as well as vehicle system vibrations. The chattering is eliminated with the introduction QFT inside the boundary layer to ensure smooth tracking. Furthermore, using SMC alone requires higher actuator forces for tracking than using both the control schemes together, and causes various problems in selecting hardware. Problems with noise amplification, resonances, presence of uncertainties, and unmodelled high-frequency dynamics can largely be avoided with the use of QFT over other optimization methods. The main contribution of the present paper is to provide guidance in designing the controller to reduce heavy vehicle seat vibration so that the driver's sensation of comfort maintains a certain level at all times.

Keywords: non-linear modelling, sliding surface, feedback control, tracking error, stability, time-varying surface, boundary layer, chattering, error dynamics, first-order filter, model uncertainty

1 INTRODUCTION

The relationship between driver fatigue and seat vibration has been used in literature based on anecdotal evidence [**1**, **2**]. It is widely believed and has been proved in field tests, that the lower vertical acceleration levels will increase the comfort level of the driver [**3–5**]. Heavy-vehicle truck drivers, who usually experience vibration levels around 3 Hz while driving, may undergo fatigue and drowsiness [**6**], which may result in lack of concentration leading to road accidents. Laboratory and field tests reveal that different road conditions can trigger higher levels of vertical accelerations [**1–6**]. In addition, human body metabolism and chemistry can largely be affected owing to intermittent and random vibration exposure resulting in fatigue [**7**]. Typically, vibration exposure levels of heavy-vehicle drivers are in the range 0.4–2.0 m/s^2 with a mean value of 0.7 m/s^2 in the vertical axis [**3–6**].

A suspension system determines the ride comfort of the vehicle and therefore its characteristics may be properly evaluated to design a proper driver seat under various operating conditions. It also improves vehicle control, safety, and stability without changing the ride quality, road holding, load carrying, and passenger comfort while providing directional control during handling manoeuvres. A properly designed driver seat can reduce driver fatigue, while maintaining the same vibration levels, against different external disturbances to provide improved performance in riding.

Over the past decades, the application of sliding mode control has been focused in many directions such as the use of sliding control in underwater vehicles, automotive applications, and robot manipulators [**8–17**]. The combination of sliding controllers with state observers was also developed and discussed for both the linear and non-linear cases

* *Corresponding author: Lennox Industries, Inc., 1600 Metrocrest Drive, Carrollton, TX 75006, USA. email: nrajapak@mail.smu.edu*

[**18**, **19**]. Non-linear systems are as difficult to model as linear systems since there are certain parametric uncertainties and modelling inaccuracies that can eventually resonate the system [**9**]. The sliding-mode control (SMC) can be used for non-linear stabilization problems in designing controllers. SMC can provide high-performance systems that are robust to parameter uncertainties and disturbances. Design of such systems includes two steps: (a) choosing a set of switching surfaces that represent some sort of a desired motion and (b) designing a discontinuous control law that ensures convergence to the switching surfaces [**11**, **12**]. The discontinuous control law guarantees the attractiveness of the switching surfaces in the phase space. Sliding mode occurs when the system trajectories are confined to the switching surfaces and cannot leave them for the remainder of the motion. Although this control approach is relatively well understood and extensively studied, important issues related to implementation and chattering behaviour remain unresolved. However, implementing the quantitative feedback theory (QFT) during the sliding phase of a SMC controller not only eliminates chatter but also achieves vibration isolation. In addition, QFT does not diminish the robustness characteristics of the SMC because it is known to tolerate large parametric and phase information uncertainties.

In the current paper, the SMC theory is applied to track the motion behaviour of a driver seat of a heavy vehicle to a trajectory that can reduce driver fatigue and drowsiness. The trajectory can be varied accordingly with respect to the driver requirements. This control methodology can overcome most of the road disturbances and provide a predetermined seat motion pattern to avoid driver fatigue. However, owing to parametric uncertainties and modelling inaccuracies, chattering can be observed which causes a major problem in applying SMC alone. In general, the chattering enhances the driver fatigue and also leads to premature failure of controllers. SMC with QFT implemented in the present paper not only eliminates the chattering satisfactorily but also reduces the control effort necessary to maintain the desired motion of the seat.

2 MATHEMATICAL MODELLING

Figure 1 shows a schematic diagram of a driver seat of a heavy truck. The model consists of an actuator, spring, damper, and a motor sitting on the sprung mass. The actuator provides actuation force by means of a hydraulic actuator to keep the seat motion within a comfort level for any road disturbance, while the motor maintains the desired inclination angle of the driver seat with respect to the roll angle of the sprung mass. The driver-seat mechanism is connected to the sprung mass by using a pivoted joint and it provides the flexibility to change the roll angle. The system is equipped with sensors to measure the sprung mass vertical acceleration and roll angle. Hydraulic pressure drop and spool valve displacement are also used as feedback signals.

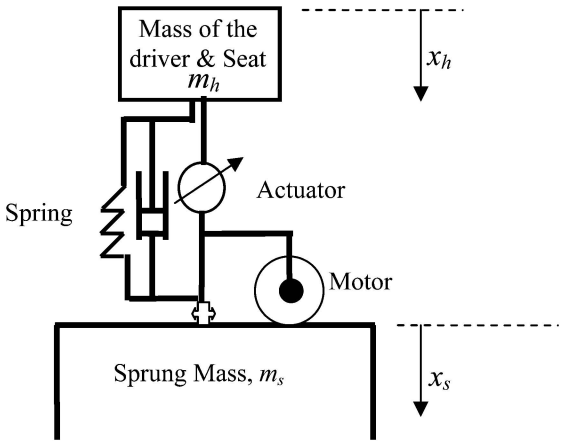

Fig. 1 The hydraulic power feed of the driver seat on the sprung mass

3 EQUATIONS OF MOTION

Based on the mathematical model developed above, the equation of motion in the vertical direction for the driver and the seat can be written as follows

$$\ddot{x}_{\mathrm{h}} = -(1/m_{\mathrm{h}})F_{\mathrm{h}} + (1/m_{\mathrm{h}})F_{\mathrm{af}} \tag{1}$$

where

$F_{\mathrm{h}} = k_{\mathrm{h}}(d_{\mathrm{h}} + d_h^3) + C_{\mathrm{h}}(1 + |\dot{d}_{\mathrm{h}}|^2)\dot{d}_{\mathrm{h}}$
$F_{\mathrm{af}} = AP_{\mathrm{L}}$
$d_{\mathrm{h}} = (x_{\mathrm{h}} - x_{\mathrm{s}}) - a_{1i}\sin\theta_{\mathrm{s}}$ (see Appendix 2 for details)

In a four-way valve–piston hydraulic actuator system, the rate of change of pressure drop across the hydraulic actuator piston, P_{L}, is given by [**20**]

$$\frac{V_{\mathrm{t}}\dot{P}_{\mathrm{L}}}{4\beta_{\mathrm{e}}} = Q - C_{\mathrm{tp}}P_{\mathrm{L}} - A(\dot{x}_{\mathrm{h}} - \dot{x}_{\mathrm{s}}) \tag{2}$$

where V_{t} is total actuator volume, β_{e} is effective bulk modulus of the fluid, Q is the load flow, C_{tp} is total piston leakage coefficient, and A is piston area.

The load flow of the actuator is given by [**20**]

$$Q = \mathrm{sgn}[P_{\mathrm{s}} - \mathrm{sgn}(x_{\mathrm{v}})P_{\mathrm{L}}] \times C_{\mathrm{d}}\omega x_{\mathrm{v}}\sqrt{(1/\rho)|P_{\mathrm{s}} - \mathrm{sgn}(x_{\mathrm{v}})P_{\mathrm{L}}|} \tag{3}$$

where P_s is hydraulic supply pressure, ω is spool valve area gradient, x_v is displacement of the spool valve, ρ is hydraulic fluid density, and C_d is the discharge coefficient.

Voltage or current can be fed to the servo-valve to control the spool valve displacement of the actuator for generating the force. Moreover, a stiction model for hydraulic spool can be included to reduce the chattering further, but it is not discussed here.

4 SLIDING-MODE CONTROL PRELIMINARIES

In SMC a time-varying surface of $S(t)$ is defined with the use of a desired vector, X_d, and the term 'sliding surface' is used. If the state vector, X, can constantly remain on the surface, $S(t)$ then $t > 0$, tracking can be achieved. In other words, the problem of tracking the state vector, $X \equiv X_d$ (n-dimensional desired vector) is solved. The scalar quantity, s, is the distance to the sliding surface and this becomes zero at the time of tracking. This replaces the vector X_d effectively by a first-order stabilization problem in s. The scalar s represents a realistic measure of tracking performance since bounds on s and the tracking error vector are directly connected together. In designing the controller, a feedback control law U can be chosen appropriately to satisfy sliding conditions. The control law across the sliding surface can be made discontinuous in order to facilitate for the presence of modelling imprecision and of disturbances. Then the discontinuous control law U is smoothed accordingly using QFT to achieve an optimal trade-off between control bandwidth and tracking precision.

Consider the second-order single-input dynamic system [**9**]

$$\ddot{x} = f(X) + b(X)U \tag{4}$$

where X is the state vector, $[x \quad \dot{x}]^T$, x is output of interest, f is non-linear time-varying or state-dependent function, b is control gain, and U is control input torque.

The control gain, b, can be time varying or state dependent but is not completely known. In other words, it is sufficient to know the bounding values of b

$$0 < b_{min} \leqslant b \leqslant b_{max} \tag{5}$$

The estimated value of the control gain, b_{es}, can be found as [**9**]

$$b_{es} = (b_{min} b_{max})^{1/2}$$

Bounds of the gain, b can be written in the form

$$\beta^{-1} \leqslant \frac{b_{es}}{b} \leqslant \beta \tag{6}$$

where

$$\beta = \left[\frac{b_{max}}{b_{min}}\right]^{1/2}$$

The non-linear function f can be estimated (f_{es}) and the estimation error on f is to be bounded by some function of the original states of f

$$|f_{es} - f| \leqslant F \tag{7}$$

In order to place the system track onto a desired trajectory $x(t) \equiv x_d(t)$, a time-varying surface, $S(t)$ in the state-space R^2 by the scalar equation $s(x; t) = s = 0$ is defined

$$s = \left(\frac{d}{dt} + \lambda\right)\bar{x} = \dot{\bar{x}} + \lambda\bar{x} \tag{8}$$

where

$\bar{X} = X - X_d = [\bar{x} \quad \dot{\bar{x}}]^T$
$\lambda =$ positive constant (first-order filter bandwidth)

When the state vector reaches the sliding surface, $S(t)$, the distance to the sliding surface, s, becomes zero. This represents the dynamics while in sliding mode, such that

$$\dot{s} = 0 \tag{9}$$

When equation (9) is satisfied, the equivalent control input, U_{eq} can be obtained as follows

$b \to b_{es}$

$b_{es} U \to U_{es}$

$f \to f_{es}$

This leads to

$$U_{es} = -f_{es} + \ddot{x}_d - \lambda\dot{\bar{x}} \tag{10}$$

and U is given by

$$U = \left(\frac{1}{b_{es}}\right)(U_{es} - k(x)\,\mathrm{sgn}(s))$$

where $k(x)$ is control discontinuity.

The control discontinuity, $k(x)$ is needed to satisfy sliding conditions with the introduction of an estimated equivalent control. However, this control discontinuity is highly dependent on the parametric uncertainty of the system. In order to satisfy sliding conditions and the system trajectories that remain

on the sliding surface, the following must be satisfied

$$\frac{1}{2}\frac{\mathrm{d}}{\mathrm{d}t}s^2 = s\dot{s} \leqslant -\eta|s| \tag{11}$$

where η is a strictly positive constant.

The control discontinuity can be found from the above inequality

$$\begin{aligned}
&s[(f - bb_{\mathrm{es}}^{-1}f_{\mathrm{es}}) + (1 - bb_{\mathrm{es}}^{-1})(-\ddot{x}_{\mathrm{d}} + \lambda\dot{\tilde{x}}) \\
&\quad - bb_{\mathrm{es}}^{-1}k(x)\,\mathrm{sgn}(s)] \leqslant -\eta|s| \\
&s[(f - bb_{\mathrm{es}}^{-1}f_{\mathrm{es}}) + (1 - bb_{\mathrm{es}}^{-1})(-\ddot{x}_{\mathrm{d}} + \lambda\dot{\tilde{x}})] \\
&\quad + \eta|s| \leqslant bb_{\mathrm{es}}^{-1}k(x)|s| \\
&k(x) \geqslant \frac{s}{|s|}[b_{\mathrm{es}}b^{-1}f - f_{\mathrm{es}} + (b_{\mathrm{es}}b^{-1} - 1)(-\ddot{x}_{\mathrm{d}} + \lambda\dot{\tilde{x}})] \\
&\qquad + b_{\mathrm{es}}b^{-1}\eta
\end{aligned}$$

For the best tracking performance, $k(x)$ must satisfy the inequality as follows

$$\begin{aligned}
k(x) &\geqslant |b_{\mathrm{es}}b^{-1}f - f_{\mathrm{es}} + (b_{\mathrm{es}}b^{-1} - 1)(-\ddot{x}_{\mathrm{d}} + \lambda\dot{\tilde{x}})| \\
&\quad + b_{\mathrm{es}}b^{-1}\eta
\end{aligned}$$

As seen from the above inequality, the value for $k(x)$ can be simplified further by rearranging f as below

$$\begin{aligned}
&f = f_{\mathrm{es}} + (f - f_{\mathrm{es}}) \qquad \text{and by using} \qquad |f_{\mathrm{es}} - f| \leqslant F \\
&k(x) \geqslant |b_{\mathrm{es}}b^{-1}(f - f_{\mathrm{es}}) + (b_{\mathrm{es}}b^{-1} - 1)(f_{\mathrm{es}} - \ddot{x}_{\mathrm{d}} + \lambda\dot{\tilde{x}})| \\
&\qquad + b_{\mathrm{es}}b^{-1}\eta \\
&k(x) \geqslant |b_{\mathrm{es}}b^{-1}(f - f_{\mathrm{es}})| + |(b_{\mathrm{es}}b^{-1} - 1)(f_{\mathrm{es}} - \ddot{x}_{\mathrm{d}} + \lambda\dot{\tilde{x}})| \\
&\qquad + b_{\mathrm{es}}b^{-1}\eta \\
&k(x) \geqslant \beta(F + \eta) + (\beta - 1)|(f_{\mathrm{es}} - \ddot{x}_{\mathrm{d}} + \lambda\dot{\tilde{x}})| \\
&k(x) \geqslant \beta(F + \eta) + (\beta - 1)|U_{\mathrm{es}}|
\end{aligned} \tag{12}$$

By choosing $k(x)$ to be large enough, sliding conditions can be guaranteed. This control discontinuity across the surface $s = 0$ increases with the increase of uncertainty of the system parameters. It is important to mention that the functions for f_{es} and F may be thought of as any measured variables external to the system and they also may depend explicitly on time.

5 REARRANGEMENT OF THE SLIDING SURFACE

The sliding condition as in the previous sections, $\dot{s} = 0$, does not necessarily provide smooth tracking performance across the sliding surface. In order to guarantee smooth tracking performance and to design an improved controller, in spite of the control discontinuity, the sliding condition can be redefined, i.e. $\dot{s} = -\alpha s$ [**8**], so that tracking of $x \to x_{\mathrm{d}}$ would achieve an exponential convergence. Here the parameter α is a positive constant. The value for α is determined by considering the tracking smoothness of the unstable system. This condition modifies U_{es} as follows.

$U_{\mathrm{es}} = -f_{\mathrm{es}} + \ddot{x}_{\mathrm{d}} - \lambda\dot{\tilde{x}} - \alpha s$ and $k(x)$ must satisfy the condition below

$$\begin{aligned}
k(x) &\geqslant |b_{\mathrm{es}}b^{-1}f - f_{\mathrm{es}} + (b_{\mathrm{es}}b^{-1} - 1)(-\ddot{x}_{\mathrm{d}} + \lambda\dot{\tilde{x}})| \\
&\quad + b_{\mathrm{es}}b^{-1}\eta - \alpha|s|
\end{aligned}$$

Further $k(x)$ can be simplified as

$$k(x) \geqslant \beta(F + \eta) + (\beta - 1)|U_{\mathrm{es}}| + (\beta - 2)\alpha|s| \tag{13}$$

Even though the tracking condition is improved, chattering of the system on the sliding surface remains as an inherent problem in SMC. This can indeed be removed by using QFT, as explained in section 6.

6 QFT CONTROLLER DESIGN

In the previous sections of sliding-mode preliminaries, designed control laws, which satisfy sliding conditions, lead to perfect tracking even with some model uncertainties. However, after reaching the boundary layer, the chattering of the controller is observed because of the discontinuity across the sliding surface. In practice this situation can lead to extreme complications when designing hardware for the controller and it can also affect a desirable performance because of the time lag of the hardware functionality. Furthermore, chattering excites undesirable high-frequency dynamics of the system. By using a QFT controller, the switching control laws can be modified to eliminate chattering in the system since a QFT controller works as a robust lowpass filter. In QFT, attractiveness of the boundary layer can be maintained for all $t > 0$ by varying the boundary layer thickness, ϕ, as follows, when

$$|s| \geqslant \phi \to \frac{1}{2}\frac{\mathrm{d}}{\mathrm{d}t}s^2 \leqslant (\dot{\phi} - \eta)|s| \quad [\mathbf{9}] \tag{14}$$

It is evident from equation (14) that the boundary layer attraction condition is guaranteed to a greater extent in the case of boundary layer contraction ($\dot{\phi} < 0$) than the boundary layer expansion ($\dot{\phi} > 0$). Equation (14) can be used to modify the control discontinuity gain, $k(x)$, to smoothen the performance by putting $\bar{k}(x)\,\mathrm{sat}(s/\phi)$ instead of $k(x)\,\mathrm{sgn}(s)$. The relationship between $\bar{k}(x)$ and $k(x)$ for the boundary

layer attraction condition can be presented for both the cases as follows

$$\dot{\phi} > 0 \rightarrow \bar{k}(x) = k(x) - \dot{\phi}/\beta^2 \tag{15}$$

$$\dot{\phi} < 0 \rightarrow \bar{k}(x) = k(x) - \dot{\phi}\beta^2 \tag{16}$$

Then the control law, U, and $\dot{s}$ become

$$U = \left(\frac{1}{b_{es}}\right)(U_{es} - \bar{k}(x)\,\mathrm{sat}(s/\phi))$$

$$\dot{s} = -bb_{es}^{-1}(\bar{k}(x)\,\mathrm{sat}(s/\phi) + \alpha s) + \Delta g(x, x_d)$$

where $\Delta g(x, x_d) = (f - bb_{es}^{-1} f_{es}) + (1 - bb_{es}^{-1})(-\ddot{x}_d + \lambda\dot{x})$.

Since $\bar{k}(x)$ and Δg are continuous in x, the system trajectories inside the boundary layer can be expressed in terms of the variable s and the desired trajectory x_d by the following relation.

Inside the boundary layer, i.e. $|s| \leqslant \phi \rightarrow \mathrm{sat}(s/\phi) = s/\phi$ and $x \rightarrow x_d$

Hence

$$\dot{s} = -\beta_d^2(\bar{k}(x_d)(s/\dot{\phi}) + \alpha s) + \Delta g(x_d) \tag{17}$$

where

$$\beta_d = \left[\frac{b_{es}(x_d)_{max}}{b_{es}(x_d)_{min}}\right]^{1/2}$$

The dynamics inside the boundary layer can be written by combining equations (15) and (16) as follows

$$\dot{\phi} > 0 \rightarrow \bar{k}(x_d) = k(x_d) - \dot{\phi}/\beta_d^2 \tag{18}$$

$$\dot{\phi} < 0 \rightarrow \bar{k}(x_d) = k(x_d) - \dot{\phi}\beta_d^2 \tag{19}$$

By taking the Laplace transform of equation (17), it can be shown that the variable s is given by the output of a first-order filter, whose dynamics entirely depend on the desired state x_d. $\Delta g(x_d)$ are the inputs to the first-order filter, but they are highly uncertain.

See Fig. 2, where P is the Laplace variable, this shows that chattering in the boundary layer owing to perturbations or uncertainty of $\Delta g(x_d)$ can satisfactorily be removed by a first-order filtering as shown in Fig. 2 as long as high-frequency unmodelled dynamics are not excited. The boundary layer thickness, ϕ, can be selected as the bandwidth of the first-order filter of having input perturbations same as that of the first-order filter from the definition of s,

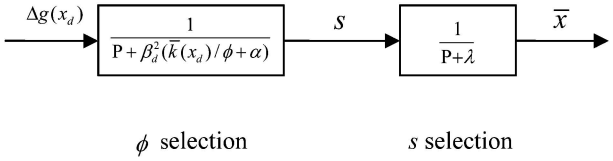

Fig. 2 Structure of the closed-loop error dynamics

which leads to tuning ϕ with λ

$$\beta_d^2[\bar{k}(x_d)/\phi + \alpha] = \lambda$$

$$\bar{k}(x_d) = (\lambda/\beta_d^2 - \alpha)\phi \tag{20}$$

Combining equations (18) and (20) yields

$$k(x_d) > \phi(\lambda/\beta_d^2 - \alpha)$$

and

$$\dot{\phi} + (\lambda - \alpha\beta_d^2)\phi = \beta_d^2 k(x_d) \tag{21}$$

Also combining equations (19) and (20) gives

$$k(x_d) < \phi(\lambda/\beta_d^2 - \alpha)$$

and

$$\dot{\phi} + (\phi/\beta_d^2)[(\lambda/\beta_d^2) - \alpha] = k(x_d)/\beta_d^2 \tag{22}$$

combining equations (15) and (21)

$$\dot{\phi} > 0 \rightarrow \bar{k}(x) = k(x) - (\beta_d/\beta)^2[k(x_d) - \phi(\lambda/\beta_d^2 - \alpha)] \tag{23}$$

and combining equation (13) with equation (19)

$$\dot{\phi} < 0 \rightarrow \bar{k}(x) = k(x) - (\beta/\beta_d)^2[k(x_d) - \phi(\lambda/\beta_d^2 - \alpha)] \tag{24}$$

In addition, the initial value of the boundary layer thickness, $\phi(0)$, is given by substituting x_d at $t = 0$ in equation (20).

$$\phi(0) = \frac{\bar{k}(x_d(0))}{(\lambda/\beta_d^2) - \alpha}$$

Sections 1–6 can be used for applications to track and stabilize highly non-linear systems. Sliding-mode control along with QFT provides better system controllers and it leads to easier selection of hardware than using SMC alone. The application of this theory to heavy-truck driver-seat and its simulation are given in the following sections.

7 APPLICATIONS AND SIMULATIONS (MATLAB)

Equation (1) can be represented as

$$\ddot{x}_h = f + bU \tag{25}$$

where

$$f = -(1/m_h)F_h$$

$$b = 1/m_h$$

$$U = F_{af}$$

The expression f is a time-varying function of x_s and the state vector, x_h. The time-varying function, x_s can be estimated from the information of the sensor, attached to the sprung mass and its limits of variation must be known. The expression f and the control gain, b, are not required to be known exactly, but their bounds should be known in applying SMC and QFT. In order to perform the simulation, x_s is assumed to vary between -0.3 m and 0.3 m and it can be approximated by the time-varying function, $A\sin(\omega t)$, where ω is the disturbance angular frequency of the road by which the unsprung mass is oscillated. The bounds of the parameters are given as follows

$$m_{hmin} \leqslant m_h \leqslant m_{hmax}$$

$$x_{smin} \leqslant x_s \leqslant x_{smax}$$

$$b_{min} \leqslant b \leqslant b_{max}$$

Estimated values of m_h and x_s

$$m_{hes} = |(m_{hmin} m_{hmax})^{1/2}|$$

$$x_{ses} = (|x_{smin} x_{smax}|)^{1/2}$$

The above bounds and the estimated values can roughly be obtained for some heavy trucks by utilizing field test information [**21–27**]. They are as follows

$$m_{hmin} = 50 \text{ kg}, \; m_{hmax} = 100 \text{ kg}$$

$$x_{smin} = -0.3 \text{ m}, \; x_{smax} = 0.3 \text{ m}, \; \omega = 2\pi(0.1 - 10) \text{ rad/s}$$

$$A = 0.3$$

The estimated non-linear function, f, and bounded estimation error, F, are given by

$$f_{es} = -(k_h/m_{hes})(x_h - x_{ses})$$

$$F = |f_{es} - f|_{max}$$

$$b_{es} = 0.014$$

$$\beta = 1.414$$

$$x_{ses} = (|(x_s)_{max} * (x_s)_{min}|)^{1/2}$$

The sprung mass is oscillated owing to road disturbances and its changing pattern is given by the vertical angular frequency, $\omega = 2\pi(0.1 + |9.9\sin(2\pi t)|)$. This function for ω is used in the simulation in order to vary the sprung mass frequency from 0.1 to 10 Hz. Thus ω can be measured by using the sensors in real time and be fed to the controller to estimate the control force necessary to maintain the desired frequency limits of the driver seat. The expected trajectory for x_h is given by the function, $x_{hd} = B\sin\omega_d t$, where ω_d is the desired angular frequency of the driver to have comfortable driving conditions to avoid driver fatigue in the long run. B and ω_d are assumed to be 0.05 m and $2\pi \times 0.5$ rad/s during the simulation, which yields 0.5 Hz continuous vibration for the driver seat over the time. The mass of the driver and seat is considered to be 70 kg throughout the simulation. This value changes from driver to driver and can be obtained by attaching the load cell to the driver seat to calculate the control force. The spring constant between the driver seat and the sprung mass is selected as 100 N/m. It is important to mention that this control scheme provides sufficient room to change the vehicle parameters of the system according to the driver requirements to achieve ride comfort.

8 USING SLIDING MODE ONLY

In this section the tracking is achieved by using SMC alone and the simulation results are obtained as follows.

Consider $x_h = x(1)\,(m)$ and $\dot{x}_h = x(2)$ (m/s). Equation (25) is represented in state space form as follows

$$\dot{x}(1) = x(2)$$

$$\dot{x}(2) = -(k_h/m_h)(x(1) - x_{ses}) + bU$$

Combining equations (8), (10), and (25), the estimated control law becomes

$$U_{es} = -f_{es} + \ddot{x}_{hd} - \lambda[x(2) - \dot{x}_{hd}]$$

Figures 3 to 6 shows system trajectories, tracking error, and control torque for the initial condition $[x_h, \dot{x}_h] = [0.1 \text{ m}, 1 \text{ m/s}]$ using the control law. Figure 3 provides the tracked vertical displacement of the driver seat versus time and perfect tracking behaviour can be observed. Figure 4 exhibits the tracking error and it is enlarged in Fig. 5 to show its chattering behaviour after the tracking is achieved. Chattering

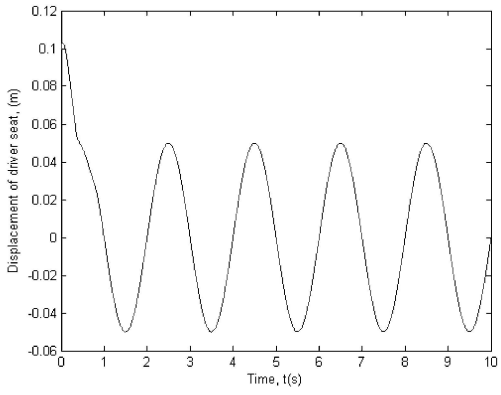

Fig. 3 Vertical displacement of driver seat versus time using SMC only

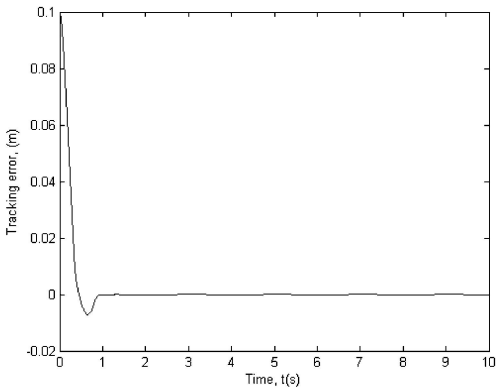

Fig. 4 Tracking error versus time using SMC only

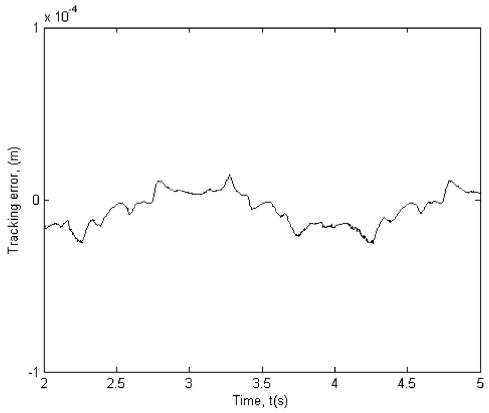

Fig. 5 Zoomed in tracking error versus time using SMC only

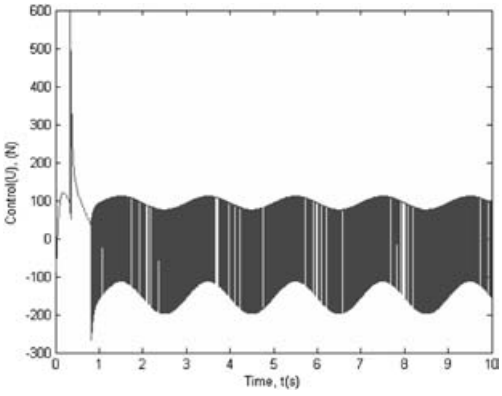

Fig. 6 Control force versus time using SMC only

is undesirable for the controller because it makes it impossible to select hardware and leads to premature failure of hardware.

The values for λ and η in equations (8) and (11) are chosen as 20 and 0.1 [**9**] to obtain the plots and to achieve satisfactory tracking performance. The sampling rate of 1 kHz is selected in the simulation. The $\dot{s} = 0$ condition and the *signum* function are used. The plot of control force versus time is given in Fig. 6. It is very important to mention that the tracking is guaranteed only with excessive control forces. The mass of the driver and driver seat, limits of its operation, control bandwidth, initial conditions, sprung mass vibrations, chattering, and system uncertainties are various factors that cause huge control forces to be generated. It should be mentioned that this selected example is governed only by the linear equations with sine disturbance function, which cause for the controller to generate periodic sinusoidal signals. In general, the road disturbance is sporadic and the smooth control action can never be expected. This will lead to chattering and QFT is needed to filter them out. Moreover, applying SMC with QFT can reduce excessive control forces and will ease the selection of hardware.

In subsequent results, the spring constant of the tyres is selected as 1200 kN/m and the damping coefficient as 300 kNs/m. Some of the trucks' numerical parameters [**8**, **12**, **21–27**] are used in obtaining plots and they are: $m_h = 100$ kg, $m_s = 3300$ kg, $m_u = 1000$ kg, $k_s = 200$ kN/m, $k_h = 1$ kN/m, $C_s = 50$ kNs/m, $C_h = 0.4$ kNs/m, $J_s = 3000$ kgm^2, $J_u = 900$ kgm^2, $A_i = 0.3$ m, $S_i = 0.9$ m, and $a_{1i} = 0.8$ m.

9 USE OF QFT ON THE SLIDING SURFACE

In order to lower the excessive control force and to further smoothen the control behaviour with a view to reduce chattering, QFT is introduced inside the boundary layer. The graphs shown in Figs 7 to 10 are plotted for the initial boundary layer thickness of 0.1 m.

Figure 7 again shows that the system is tracked to the trajectory of interest and it follows the desired trajectory of the seat motion over time. Figure 9

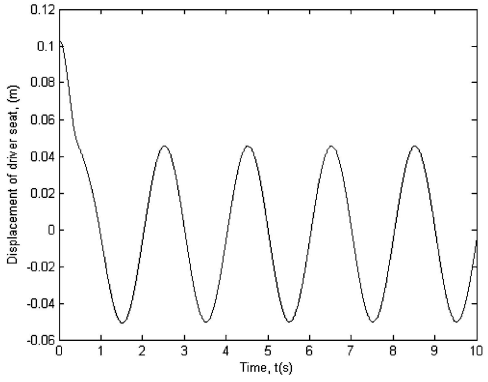

Fig. 7 Vertical displacement of driver seat versus time using SMC and QFT

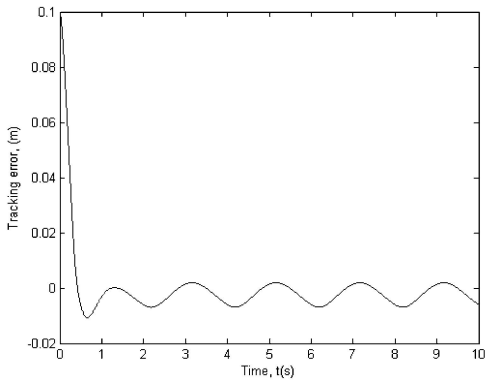

Fig. 8 Tracking error versus time using SMC and QFT

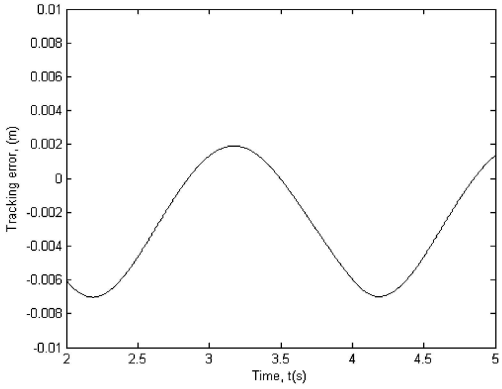

Fig. 9 Zoomed in tracking error versus time using SMC and QFT

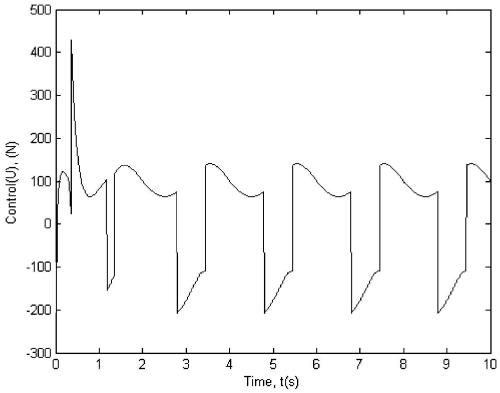

Fig. 10 Control force versus time using SMC and QFT

provides zoomed in tracking error of Fig. 8, which is very small and a perfect tracking condition is achieved. The control force needed to track the system is given in Fig. 10. Figure 11 provides control forces for both the cases, i.e. SMC with QFT and SMC alone. SMC with QFT yields lower control force and this can precisely be generated by using a hydraulic

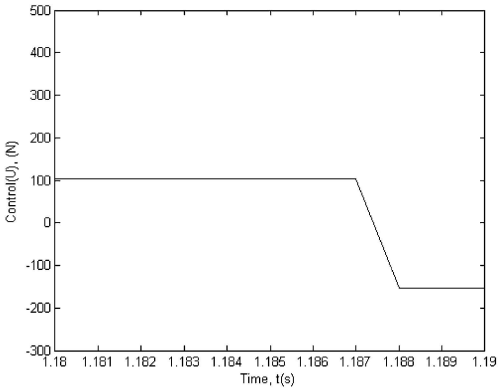

Fig. 11 Zoomed in control force versus time using SMC and QFT

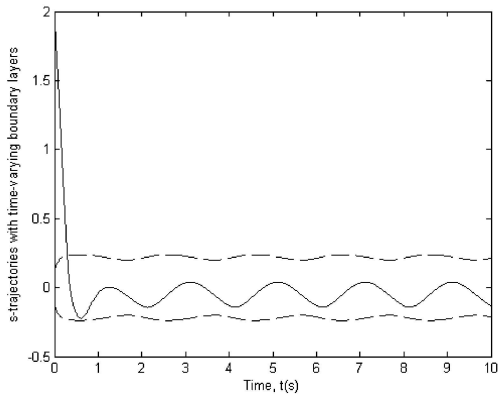

Fig. 12 s-trajectory with time-varying boundary layer versus time using SMC and QFT

actuator. Increasing the parameter λ will decrease the tracking error with the increase of initial control effort.

Varying thickness of the boundary layer allows for the better use of the available bandwidth, which causes the control effort for tracking the system to be reduced. Parameter uncertainties can effectively be addressed and the control force can be smoothened with the use of both the SMC and QFT rather than applying SMC alone. A successful application of QFT methodology requires selecting a suitable function for F, since the change in boundary layer thickness is dependent on the bounds of F. Increases in the bounds of F will increase the boundary layer thickness that leads to an overestimation of the change in boundary layer thickness and the control effort. Evolution of dynamic model uncertainty with time is given by the change of boundary layer thickness. The correct selection of the parameters and their bounds always results in lower tracking errors and control forces, which will ease choosing hardware for most of the applications.

10 CONCLUSIONS

The current paper presents information for designing a road-adaptive driver seat of a heavy truck via a combination of SMC and QFT. Based on the assumptions, the simulation results show that the adaptive driver-seat controller has high potential to provide a superior driver comfort over a wide range of road disturbances. However, parameter uncertainties, the presence of unmodelled dynamics such as structural resonant modes, neglected time-delays, and finite sampling rate can largely change the dynamics of such systems. SMC provides an effective methodology to design and test the controllers in the performance trade-offs, thus the tracking is guaranteed within the operating limits of the system. Combined use of SMC and QFT facilitates the controller to behave smoothly and with minimum chattering that is an inherent obstacle of using SMC alone. Chattering reduction by the use of QFT enables to select hardware in the realistic range, avoiding over design since the excessive control action is satisfactorily eliminated. In this paper simulation study is done for a linear system with sinusoidal disturbance inputs. It is seen that very high control effort is needed owing to fast switching behaviour in the case of using SMC alone. QFT smoothens the switching nature and the control effort can be minimized. Most of the controllers fail when excessive chattering is present and SMC with QFT can be used effectively to smoothen the control action. In this example the control gain is independent of the states, $x(1)$ and $x(2)$ and it has a fixed value. This will ease the control manipulation. The developed theory can be used effectively in most of the control problems to reduce chattering and to lower the control effort. It should be mentioned here that the acceleration feedback is not always needed for position control, since it depends mainly on the control methodology and the system employed. In order to implement the control law, the road disturbance frequency, ω, should be measured at a rate higher or equal to 1000 Hz (just to comply with the simulation requirements) to update the system, but the higher the better. The bandwidth of the actuator depends upon several factors, i.e. how quickly the actuator can generate the force needed, road profile, response time, signal delay, etc.

Driver fatigue is a contributing factor in between 4 per cent to 30 per cent of road crashes and the low-frequency vibrations in heavy vehicles are mostly caused by the long wavelengths of the road surface [**3**, **6**]. These wavelengths occur on roads, creating an undulating effect. Valuable scientific data on physiological and psychological effects are needed to develop guidelines for better truck seat designs. This approach can easily be adopted for most of the designs and could provide satisfactory results to reduce driver fatigue and drowsiness.

REFERENCES

1 **Wilson, L. J.** and **Horner, T. W.** *Data analysis of tractor-trailer drivers to assess drivers' perception of heavy duty truck ride quality. Report DOT-HS-805-139*. 1979 (National Technical Information Service, Springfield, VA, USA).

2 **Randall, J. M.** Human subjective response to lorry vibration: implications for farm animal transport. *J. Agric. Engng, Res.*, 1992, **52**, 295–307.

3 **Landstrom, U.** and **Landstrom, R.** Changes in wakefulness during exposure to whole body vibration. *Electroencephal, Clin., Neurophysiol.*, 1985, **61**, 411–115.

4 **Altunel, A. O.** *The effect of low-tire pressure on the performance of forest products transportation vehicles*. Master's thesis, Louisiana State University, School of Forestry, Wildlife and Fisheries, 1996.

5 **Altunel, A. O.** and **de Hoop, C. F.** *The effect of lowered tire pressure on a log truck driver seat*, Vol. 9, no. 2, 1998, Louisiana State University Agricultural Center, Baton Rouge, USA.

6 **Mabbott, N., Foster, G.,** and **Mcphee, B.** Heavy vehicle seat vibration and driver fatigue. *Report no. CR 203*, 2001, p. 35 (Australian Transport Safety Bureau, Canberra City).

7 **Kamenskii, Y.** and **Nosova, I. M.** Effect of whole body vibration on certain indicators of neuro-endocrine processes. *Noise Vibration Bull.*, 1989, 205–206.

8 **Taha, E. Z., Happawana, G. S.,** and **Hurmuzlu, Y.** Quantitative feedback theory (QFT) for chattering reduction and improved tracking in sliding mode control (SMC). *ASME J. Dynamic Systems, Measmnt, Control*, 2003, **125**, 665–669.

9 **Jean-Jacques, E. S.** and **Weiping, L.** *Applied nonlinear control*, 1991 (Prentice-Hall, Englewood Cliffs, New Jersey).

10 **Roberge, J. K.** *The mechanical seal*. Bachelor's thesis, Massachusetts Institute of Technology, 1960.

11 **Dorf, R. C.** *Modern control systems*, 1967, pp. 276–279 (Addison-Wesley, Reading, Massachusetts).

12 **Ogata, K.** *Modern control engineering*, 1970, pp. 277–279 (Prentice-Hall, Englewood Cliffs, New Jersey).

13 **Higdon, D. T.** and **Cannon, R. H.** On the control of unstable multiple-output mechanical systems. ASME publications 63-WA-48, 1963, pp. 1–12.

14 **Truxal, J. G.** *State models, transfer functions, and simulation*, monograph 8, Discrete Systems Concept Project, 1965.

15 **Lundberg, K. H.** and **Roberge, J. K.** Classical dual-inverted-pendulum control. In Proceeding of the IEEE *CDC 2003*, Maui, Hawaii, 2003, pp. 4399–4404.

16 Phillips, L. C. *Control of a dual inverted pendulum system using linear-quadratic and H-infinity methods*. Master's thesis, Massachusetts Institute of Technology, 1994.

17 Siebert, W. McC. *Circuits, signals, and systems*, 1986 (MIT Press, Cambridge, Massachusetts).

18 Hedrick, J. K. and **Gopalswamy, S.** Nonlinear flight control design via sliding method, Department of Mechanical Engineering, University of California, Berkely, 1989.

19 Bondarev, A. G., Bondarev, S. A., Kostylyova, N. Y., and **Utkin, V. I.** Sliding modes in systems with asymptotic state observers. *Autom. Remote Control*, 1985, **6**.

20 Tabarrok, B. and **Tong, X.** Directional stability analysis of logging trucks by a yaw roll model. Technical Reports, University of Victoria, Mechanical Engineering Department, 1993, pp. 57–62.

21 Esmailzadeh, E., Tong, L., and **Tabarrok, B.** Road vehicle dynamics of log hauling combination trucks. SAE paper 912670, 1990, pp. 453–466.

22 Tabarrok, B. and **Tong, L.** The directional stability analysis of log hauling truck – double doglogger. Technical Reports, University of Victoria, Mechanical Engineering Department, 1992, DSC-Vol. 44, pp. 383–396.

23 Aksionov, P. V. Law and criterion for evaluation of optimum power distribution to vehicle wheels. *Int. J. Vehicle Des.*, 2001, **25**(3), 198–202.

24 Gillespie, T. D. *Fundamentals of vehicle dynamics*, 1992 (Society of Automobile Engineers, Warrendale, PA).

25 Wong, J. Y. *Theory of ground vehicles*, 1978 (John Wiley, New York).

26 Rajapakse, N. and **Happawana, G. S.** A nonlinear six degree-of-freedom axle and body combination roll model for heavy trucks' directional stability. In Proceedings of IMECE2004-61851, ASME International Mechanical Engineering Congress and RD&D Exposition, 13–19 November, Anaheim, California, USA, 2004.

27 Fialho, I. and **Balas, G. J.** Road adaptive active suspension design using linear parameter-varying gain-scheduling. *IEEE Trans. Control Systems Technol.*, 2002, **10**(1), 43–54.

APPENDIX 1

Notation

A cross-sectional area of the hydraulic actuator piston
F_{af} actuator force
F_h combined nonlinear spring and damper force of the driver seat
k_h stiffness of the spring between the seat and the sprung mass
m_h mass of the driver and the seat
m_s sprung mass
x_h vertical position coordinate of the driver seat
x_s vertical position coordinate of the sprung mass

APPENDIX 2

Common equation for representing non-linear force

Non-linear tyre forces, suspension forces, and driver-seat forces can be obtained by substituting appropriate coefficients to the following non-linear equation that covers a wide range of operating conditions for representing dynamical behaviour of the system

$$F = k(d + d^3) + C(1 + |\dot{d}|^2)\dot{d}$$

where F represents force, k is spring constant, C is damping coefficient, d is deflection, and $\dot{d}$ is rate of change of deflection.

For the suspension

$$F_{si} = k_{si}(d_{si} + d_{si}^3) + C_{si}(1 + |\dot{d}_{si}|^2)\dot{d}_{si} \qquad i = 1, 2$$

For the tyres

$$F_{ti} = k_{ti}(d_{ti} + d_{ti}^3) + C_{ti}(1 + |\dot{d}_{ti}|^2)\dot{d}_{ti} \qquad i = 1, 2, 3, 4$$

For the seat

$$F_h = k_h(d_h + d_h^3) + C_h(1 + |\dot{d}_h|^2)\dot{d}_h$$

Deflection of the suspension springs and dampers

Based on the mathematical model developed, deflection of the suspension system on the axle is found for both sides as follows:

Deflection of side 1

$$d_{s1} = (x_s - x_u) + S_i(\sin\theta_s - \sin\theta_u)$$

Deflection of side 2

$$d_{s2} = (x_s - x_u) - S_i(\sin\theta_s - \sin\theta_u)$$

Deflection of the seat springs and dampers

By considering the free body diagram in Fig. 13, deflection of the seat is obtained as follows [**27**]

$$d_h = (x_h - x_s) - a_{1i}\sin\theta_s$$

Tyre deflections

The tyres are modelled by using springs and dampers. Deflections of the tyres to a road disturbance are given by the following equations.

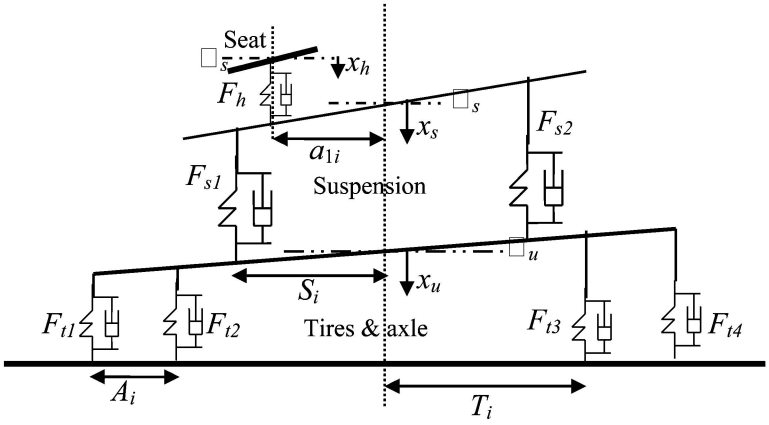

Fig. 13 Five-degree-of-freedom roll and bounce motion configuration of the system to a sudden impact

Deflection of tyre 1

$$d_{t1} = x_u + (T_i + A_i) \sin \theta_u$$

Deflection of tyre 2

$$d_{t2} = x_u + T_i \sin \theta_u$$

Deflection of tyre 3

$$d_{t3} = x_u - T_i \sin \theta_u$$

Deflection of tyre 4

$$d_{t4} = x_u - (T_i + A_i) \sin \theta_u$$

Equations of motion

Based on the mathematical model developed above, the equations of motion for each of the sprung mass, unsprung mass, and the seat are written by utilizing the free-body diagram of the system in Fig. 13 as follows.

Vertical and roll motion for the *i*th axle (unsprung mass)

$$m_u \ddot{x}_u = (F_{s1} + F_{s2}) - (F_{t1} + F_{t2} + F_{t3} + F_{t4}) \tag{26}$$

$$J_u \ddot{\theta}_u = S_i(F_{s1} - F_{s2}) \cos \theta_u + T_i(F_{t3} - F_{t2}) \cos \theta_u + (T_i + A_i)(F_{t4} - F_{t1}) \cos \theta_u \tag{27}$$

Vertical and roll motion for the sprung mass

$$m_s \ddot{x}_s = -(F_{s1} + F_{s2}) + F_h \tag{28}$$

$$J_s \ddot{\theta}_s = S_i(F_{s2} - F_{s1}) \cos \theta_s + a_{1i} F_h \cos \theta_s \tag{29}$$

Vertical motion for the seat

$$m_h \ddot{x}_h = -F_h \tag{30}$$

Equations (26) to (30) have to be solved simultaneously, since there exist many parameters and non-linearities. Non-linear effects can better be understood by varying the parameters and examining relevant dynamical behaviour, since changes in parameters change the dynamics of the system. Furthermore, equations (26) to (30) can be represented in the phase plane, while varying the parameters of the truck, since each and every trajectory in the phase portrait characterizes the state of the truck. Equations above can be converted to the state space form and the solutions can be obtained using MATLAB. Phase portraits are used to observe the non-linear effects with the change of the parameters. A change in the initial conditions clearly changes the phase portraits and the important effects on the dynamical behaviour of the truck can be understood.